Effect of microstructure on heat transfer through compacted cement-stabilised soils

Document Version:
Peer reviewed version

Published In:
Geomechanics from Micro to Macro, Vols I and II

Effect of microstructure on heat transfer through compacted cement-stabilised soils

C. Beckett & D. Ciancio
School of Civil, Environmental and Mining Engineering
University of Western Australia, Australia.

ABSTRACT: Recent work has identified that the compaction of cement-stabilised soils at water contents above and below their optimum value significantly affects material strength due to the creation of contrasting microstructures. Besides strength, however, it is also likely that these materials will have different thermal properties, due to the different arrangement of particles and aggregates. These differences cannot be predicted by current methods due to their reliance on material phase volume fractions, rather than distributions. This is of particular importance to the rammed earth (RE) construction industry, a popular form of environmentally-friendly construction in Australia. RE is currently penalised under Australian building regulations due to its apparently-poor thermal properties. The ability to engineer, or at least better predict, the thermal properties of these materials will therefore be of significant benefit.

This paper presents results for the development and validation of the experimental equipment and procedures necessary to determine the thermal properties of cement-stabilised RE (CSRE) materials. The development of sensors able to be incorporated into CSRE materials is discussed and two installation methods — embedding and drilling-and-grouting — are investigated using specimens of constant microstructure as confirmed via Scanning Electron Microscope (SEM) analysis. Results show that preparation techniques were able to produce consistent microstructures and that little difference is found between calculated thermal properties (thermal resistance and specific heat capacity) for either installation technique. However, calculated thermal properties differ significantly from those found by previous authors. Further testing will therefore be conducted to investigate this shortfall, prior to the extension of this work to additional materials and microstructures.

1   INTRODUCTION

In one dimension, heat transfer through solids under unsteady conditions is governed by thermal gradient and thermal diffusivity, α, as given by:

$$\frac{\partial T}{\partial t} = \alpha \frac{\partial^2 T}{\partial x^2} = \frac{k}{\rho C_p}\left(\frac{\partial^2 T}{\partial x^2}\right) \qquad (1)$$

where T is temperature, t is time, x is the length-wise coordinate of the solid medium, k is the thermal resistance, ρ is the material bulk density, C_p is the specific heat capacity and ρC_p is the "thermal mass", that is the ability of the material to absorb and store heat (Rohsenow & Choi 1961). Eqn 1 can be extended to soils by considering the contribution of each individual material phase (soil minerals, pore fluids etc.) to the overall thermal properties according to their respective volume fractions, for example

$$C_p^* = \sum_{i=1 \to n} C_{p_i}\theta_i \qquad (2)$$

for overall specific heat capacity (C_p^*), where i is the material phase in question and θ_i is its volume fraction (Hillel 1998). The advantages of this technique are: *i)* that it is generally a straightforward process to identify individual principal phase volume fractions and; *ii)* that it offers a simple method to predict changes in thermal properties due to changes in their phase quantities. It is unable to account for the *distributions* of those phases, however, instead assuming that all phases are able to affect thermal properties equally. More advanced techniques (e.g. Nield & Bejan (2013)) are available to predict heat flow through various pore structures, however these techniques require an intimate knowledge of the material microstructure which is generally neither straightforward nor useful in practice.

Recent work conducted by Beckett & Ciancio (2014) demonstrated that contrasting microstructures can result from the compaction of cement-stabilised rammed earth (CSRE), a popular form of environmentally-friendly construction in Australia, at water contents below or above its optimum value. Be-

low optimum, the microstructure was characterised by large interaggregate pores with soil aggregates bonded by hydrated cement bridges. Above optimum, interaggregate pores were no longer evident and soil aggregates were instead inundated by a hydrated cement/fine particle matrix. Preparing the material below its optimum water content also resulted in material compressive strengths twice those when prepared above, due to the improved effectiveness of the cement bonding. However, it is reasonable to assume that these different microstructures will also result in changes in material thermal properties, due to the prevalence or absence of large pores, so that it might be that optimising one material property is detrimental to another. This is of concern to the RE construction industry, as RE's low thermal resistance means that it is generally considered unsuitable for construction by current Australian building regulations. The ability to engineer its thermal properties, by understanding their connection to material microstructure, might serve to alleviate some of these concerns and so promote the use of RE as an alternative to less sustainable construction materials, for example fired brick and concrete.

An investigation will therefore be conducted which aims to:

i) develop experimental apparatus for the testing of thermal properties of CSRE materials;

ii) determine the contribution of differing microstructural features to material thermal properties.

This paper presents results for the intermediate aim of the development and validation of the necessary experimental equipment and procedures, using a single material microstructure. Thermal data are analysed using non-steady state heat transfer theory and Scanning Electron Microscope (SEM) micrographs are also used to confirm microstructural features. This investigation forms part of a larger project, investigating the thermal performance of RE structures, with an aim to better predict occupant thermal comfort.

2 EXPERIMENTAL PROCEDURE

2.1 *Material preparation*

Specimens were manufactured from crushed limestone, commonly used for RE construction in Western Australia due to its ready availability and high degree of quality control. The material also contains very little clay, which might otherwise interfere with the cement hydration process and so offers improved material consistency over the use of natural soil (Fernandes, Purnell, Still, & Thomas 2007). Crushed limestone was sieved to remove particles larger than 10mm (necessary to facilitate compaction) and dried at 105°C for 24 hours. The dried material was then
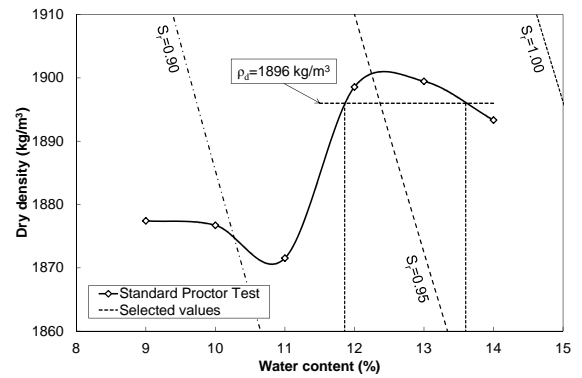

Figure 1: Compaction testing and OWC results for crushed limestone

mixed with 5% Portland cement by mass, reflecting site practice and to be in keeping with materials used in Beckett & Ciancio (2014).

Material optimum water content (OWC) was determined using the Modified Proctor Test (SA 2003), deemed to be the most representative of compactive efforts used on site (Smith & Augarde 2013). Due to the use of cement, oven-drying post compaction testing was not possible, due to the acceleration of cement hydration (Beckett & Ciancio 2014). Instead, an *a priori*-known quantity of water $w\%$ was added to the dry material and mixed for a minimum of five minutes to ensure a uniform (as much as practicable) distribution. Post-compaction water content was assumed to equal w for means of dry density calculation, as shown in Figure 1.

For the full investigation, materials prepared to a constant dry density at water contents above and below the optimum water content will be used to investigate the contribution of microstructural features to the development of material thermal properties. The need to consider constant dry density is due to the contribution of density to both thermal mass and thermal resistance, as well as to maintain, as far as possible, similar material phase volume fractions Farouki (1981). A target dry density of 1896 kg/m^3 was therefore selected, with corresponding compaction water contents of 13.6 and 11.9% for above and below-optimum materials respectively, as shown in Figure 1. For testing reported in this paper, only material prepared below the OWC (i.e. at 11.9%) will be considered for purposes of equipment validation.

2.2 *Embedded sensors and specimen manufacture*

In-house "strip" sensors were developed in collaboration with researchers at the University of Western Australia and the University of Applied Sciences, Mannheim as part of the larger project investigating thermal comfort in RE structures. These sensors can be embedded into RE walls during the ramming process to enable high-resolution temperature monitoring throughout the wall thickness. The advantage of this technique is that, as strips are embedded rather than
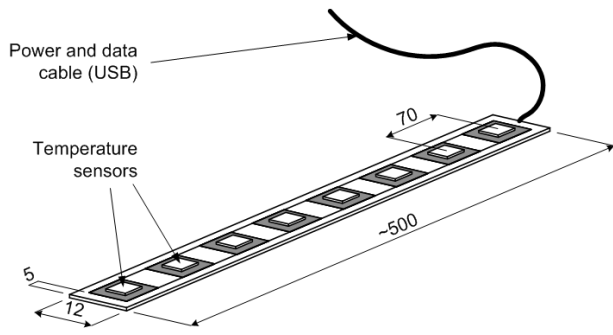
Figure 2: Sketch of the strip sensors used in preliminary testing, showing principal dimensions (in mm, not to scale)
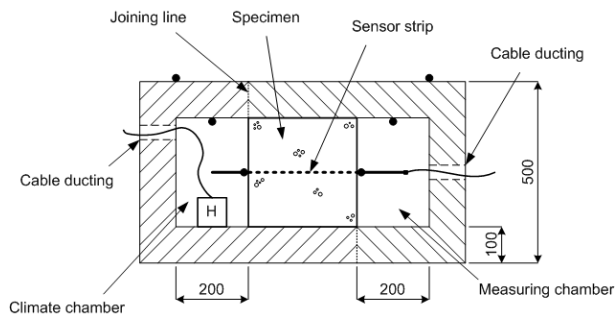

Figure 3: Sectional view of the scaled hotbox, showing principal dimensions (in mm). H = heater.

drilled, they offer a non-invasive, invisible method to monitor heat flow through the material. A sketch of the strips used in this investigation is shown in Figure 2. Strips comprise several individual temperature sensors, the number of which can be increased or decreased depending on the resolution required. Strips are covered in matte black heat shrinking material to provide a waterproof coating and to protect against penetration damage which might occur during compaction, as well as to eliminate air pockets between the sensors and the surrounding material.

A scaled "hotbox" was developed for testing CSRE specimens, based on apparatus detailed in ASTM-C1363-11 (ASTM 2011). A sketch of the hotbox is shown in Figure 3, showing principal dimensions. The hotbox comprises a "climate chamber" (CC) and a "measuring chamber" (MC), separated by the specimen with the former containing a 250W enclosure heater. The box walls are made from 100mm thick XPS Blueboard (insulating foam, extruded polystyrene), designed to be able to split in half (along the indicated joining lines) for ease of access. Sealable ducts are also provided for heater and sensor cable access. Temperature sensors were placed within the box to monitor CC and MC air temperatures, specimen wall temperatures and external air temperatures, as indicated by the black circles in Figure 3.

300mm cube CSRE specimens were manufactured for hotbox analysis. Dry limestone-cement mixture was wetted to the required water content as per compaction testing and compacted in layers of 25mm of sufficient mass to achieve the target dry density using a flat-headed electric rammer. The upper surface of each layer was scarified prior to the compaction of the overlying layer to improve inter-layer bonding.
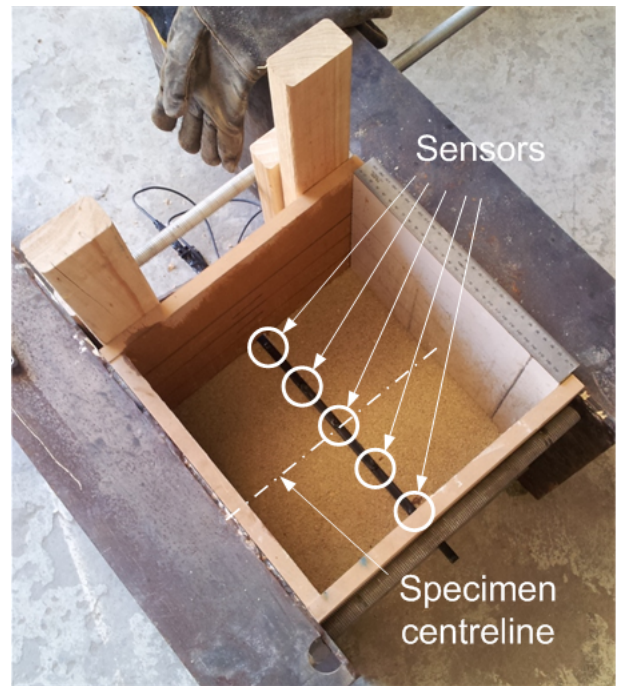

Figure 4: Positioning of the embedded strip

Once manufactured, the specimen was left to cure in a humid environment for 48 hours to ensure sufficient strength prior to removal of the formwork. It was then transferred to a drying rack and cured for a further 26 days at 94±2% relative humidity and 21±1°C.

Two methods of sensor installation were investigated: embedding (EMB) and drilling-and-grouting (DG). The former is possible for sensor installation during construction, whilst the latter is required for sensors being installed post-construction, i.e. in existing buildings where heat flows need to be monitored. For the embedded strip, specimen manufacture was paused at a depth of 150mm to enable the strip inserted through the mould, such that 5 of the 8 temperature sensors resided within the specimen, equidistant about the specimen centreline as shown in Figure 4. For drilled-and-grouted strips, a 16mm diameter hole was bored through the centre of the specimen following curing, parallel to the compaction planes. The strip was then inserted and a grout, comprising the same mix material (sieved to remove particles larger than 1.18mm), used to secure it in position. Grout was allowed to set for 24 hours prior to testing. One specimen was prepared per installation technique.

2.3 Hotbox testing

A thin layer of kaolin slurry was used to ensure good sealing between the specimens and the base, sides and top of the hotbox. Kaolin slurry was also used to seal all joins once the two halves of the box had been closed, as well as to provide additional sealing to the cable ducts. The slurry was allowed to dry for 24 hours prior to testing and temperatures were monitored during this time to ensure equilibrium between the CC and MC. The heater was then activated and CC air temperature increased to a nominal 70±1°C

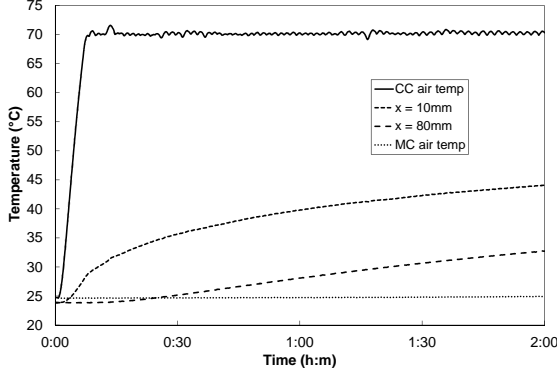Figure 5: Results for hotbox testing of EMB strips (test 1 of 2)

Figure 6: Results for hotbox testing of DG strips (test 1 of 2)

for 2 hours. The box was then allowed to cool and reach equilibrium prior to the test being repeated. On completion of the second test, the box was unsealed and the specimens cleaved along their central compaction plane to collect samples for SEM analysis. Samples of nominal size 5mm were taken from material away from any edges (strip or specimen edges) to ensure that they were representative of the specimen bulk material. Samples were then dried, coated with a 6nm layer of platinum and stored in a desiccator until needed.

Figure 7: Comparison of EMB and DG test results showing normalised temperatures

3 RESULTS AND DISCUSSION

Results for EMB and DG strips are shown in Figures 5 and 6, where x is the depth of the sensor into the specimen. Note that only sensors which showed significant temperature changes during the test are shown, and that sensor x values varied between the EMB and DG specimens due to differences in the installation techniques. A comparison between EMB and DG results is shown in Figure 7, where temperatures have been normalised via $\dfrac{\Delta T}{\Delta T_{max}}$ (where $\Delta T = T - T_i$, $\Delta T_{max} = T_f - T_i$, T_i is the initial specimen temperature and T_f is the average steady-state air temperature) to account for differences in T_i and T_f between tests. For each test, results for CC and MC air temperatures were confirmed by the box-mounted sensors, demonstrating that the temperatures within the CC and MC were relatively uniform (due to the different sensor locations) throughout the test and that the kaolin slurry was successful in providing a seal between the CC and MC.

Material thermal properties (k and C_p) can be determined from results shown in Figures 5 and 6 using the 1-D heat equation solution for heat transfer into a semi-infinite body exposed to a sudden increase in
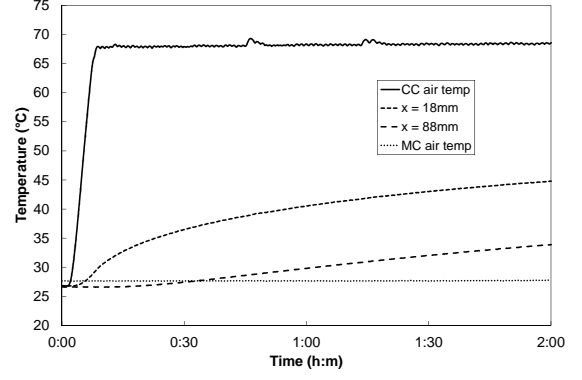
temperature (in the presence of convection), given by:

$$\frac{T - T_i}{T_f - T_i} = \mathrm{erfc}\,(X)$$

$$- \exp\left(\frac{xh}{k} + A\right)\mathrm{erfc}\left(X + \sqrt{A}\right)$$

(3)

where T is the temperature at time t, $X = \dfrac{x}{2\sqrt{\alpha t}}$, $A = \dfrac{\alpha t}{\left(\frac{k}{h}\right)^2}$, α is the thermal diffusivity (as before), h is the heat transfer coefficient for air at temperature T_f and erfc is the complementary error function. The use of Eqn 3 is valid assuming that:

i) the specimen is of sufficient size to be considered semi-infinite with respect to the embedded depth of the sensor;

ii) heat transfer is parallel to the lengthwise direction of the strip at all locations (i.e. no loss to the environment);

iii) T_f is uniform throughout the CC;

iv) the CC is of sufficient size to allow for full conduction and convection and;

v) the time required to reach maximum temperature is negligible with respect to the testing duration.
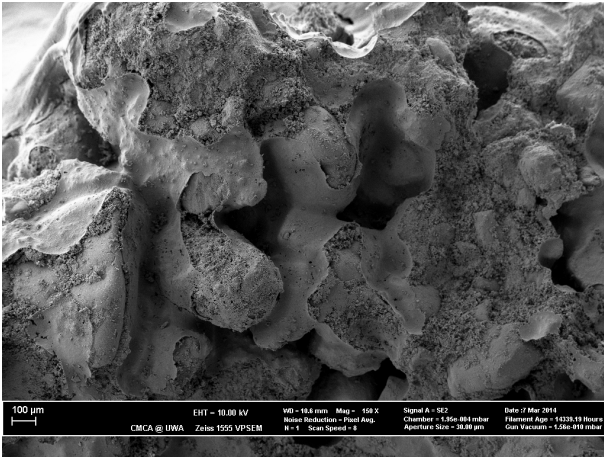
Figure 8: SEM micrograph of EMB specimen material (for image information, readers are referred to the electronic version of this article)
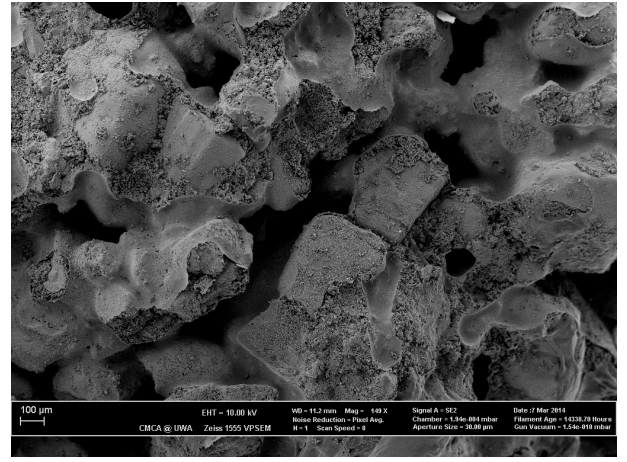

Figure 9: SEM micrograph of DG specimen material (for image information, readers are referred to the electronic version of this article)

Eqn 3 is similar to that used in ASTM-D5334 (ASTM 2008) to determine α from 1-D heat conduction into a specimen, supplied by a heat source in contact with the specimen surface, given by

$$\frac{T - T_i}{T_f - T_i} = \text{erfc}\left(X\right). \tag{4}$$

The advantage of the use of Eqn 3 over that of 4 is that values for k and C_p can be determined directly, due to the contribution of convection, whereas only α can be found using Eqn 4. Eqn 3 therefore offers a convenient method to determine material thermal properties from a single test.

Values of k and C_p found using Eqn 3 (via a least-squares fitting) are given in Table 1 for sensor depths shown in Figures 5 to 7. Note that values of ρ given in Table 1 differ from the target dry density values; this is due to the hydration of cement during curing. Table 1 shows that very similar values of k and C_p were found for the two materials at all tested depths, indicating that both methods of strip installation are acceptable for monitoring of heat flow through CSRE. This result is supported by SEM micrographs of material samples (Figures 8 and 9, both captured at the same image scale), which show that the EMB and DG specimens share almost identical microstructures; both are characterised by soil particles/aggregates separated by large interaggregate pores of approximate nominal size 100–500μm. Figures 8 and 9 also show cement bridging between particles/aggregates, with some cement gel covering particle/aggregate surfaces, as was found in (Beckett & Ciancio 2014). Figures 8 and 9 therefore confirm that material/specimen preparation techniques used here are appropriate for controlling final material microstructure.

Although Table 1 shows that repeatable results for k and C_p can be found using the scaled hotbox and Eqn 3, these values are significantly lower (roughly one third) than values found by previous authors for thermal properties of CSRE (e.g. Hall & Allinson (2009)). A sensitivity analysis was therefore conducted to determine the effects of changes in values
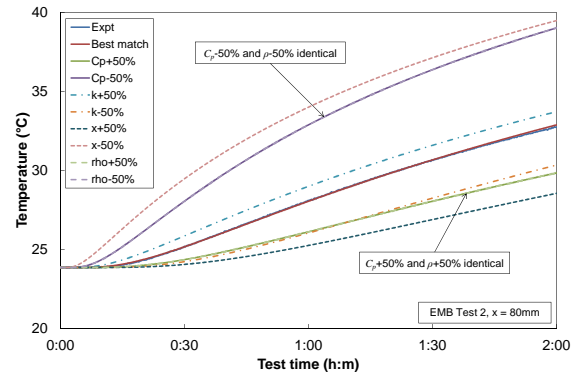

Figure 10: Sensitivity analysis for EMB results at $x = 0.08$m

of k, C_p, x and ρ on the quality of the fit of Eqn 3 to measured data, as shown in Figure 10 for the EMB specimen at $x = 0.08$m.

Figure 10 shows that Eqn 3 gives an excellent match to the experimental data, with the exception of the first few minutes due to the initial CC air temperature increase. Figure 10 also shows that temperatures predicted via Eqn 3 are quite sensitive to inaccuracies in all of the investigated variables, so that confidence in the values given in Table 1 is high. The disparity between calculated and literature results is therefore likely to be due to a violation of one, or more, of the governing assumptions behind the use of Eqn 3. For example, heat loss to the environment during testing would contravene the one-dimensional heat flow requirement; such heat loss would not necessarily be detected as a drop in CC air temperature, but rather an increased frequency with with the CC heater was activated. Further testing is therefore required in order to determine thermal properties (for example the "hot needle" test for k (ASTM 2008)) and the sources of these losses, in order to more appropriately apply Eqn 3 to measured data. Results of this testing will be reported in a subsequent paper.

Table 1: Thermal properties determined for LOWC and OWC specimens (C_p given in J/kgK, k in W/mK)

	Input parameters				Test 1		Test 2		Average values	
Specimen	x (m)	ρ (kg/m^3)	T_i (°C)	T_f (°C)	C_p	k	C_p	k	C_p	k
EMB	0.01	1986.0	23.7	68.6	315	0.45	-	-		
EMB	0.01	1986.0	23.9	70.2	-	-	324	0.34		
EMB	0.08	1986.0	23.7	68.6	276	0.42	-	-	292	0.40
EMB	0.08	1986.0	23.9	70.2	-	-	252	0.4		
DG	0.018	1955.2	24.5	68.6	260	0.40	-	-		
DG	0.018	1955.2	26.8	68.6	-	-	252	0.40		
DG	0.088	1955.2	24.0	68.6	260	0.46	-	-	261	0.43
DG	0.088	1955.2	26.6	68.6	-	-	272	0.46		

4 CONCLUSIONS

This paper has presented results for the development and validation of experimental equipment and sensor installation procedures used to determine thermal properties (k and C_p) of a CSRE material prepared below its OWC. Methods to determine k and C_p from experimental data were also examined.

Results showed that both tested specimens had similar thermal properties and that scaled hotbox testing was able to produce repeatable results for both sensor installation methods, suggesting that either method is suitable for investigating heat transfer through CSRE materials. This was supported by SEM material micrographs which showed that both materials shared almost identical microstructures, demonstrating that specific microstructres can be produced by material preparation techniques used here. However, calculated k and C_p values were roughly one third of those found by previous authors for similar materials. Additional testing is therefore required to determine the source of this shortfall, results of which will be reported in a subsequent paper.

5 ACKNOWLEDGEMENTS

REFERENCES

ASTM (2008). ASTM D5334-08. Standard test method for determination of thermal conductivity of soil and soft rock by thermal needle probe procedure.

ASTM (2011). ASTM C1363-11. Standard test method for thermal performance of building materials and envelope assemblies by means of a hot box apparatus.

Beckett, C. & D. Ciancio (2014). Effect of compaction water content on the strength of cement-stabilised rammed earth materials. *Canadian Geotechnical Journal 51*(5), 583–590.

Farouki, O. T. (1981). Thermal properties of soils. Technical report, United States Army Corps of Engineers, Cold Regions Research and Engineering Laboratory, Hanover, New Hampshire (USA).

Fernandes, V., P. Purnell, G. Still, & T. Thomas (2007). The effect of clay content in sands used for cementitious materials in developing countries. *Cement and Concrete Research 37*(5), 751–758.

Hall, M. & D. Allinson (2009). Analysis of the hygrothermal functional properties of stabilised rammed earth materials. *Building and Environment 44*(9), 1935–1942.

Hillel, D. (1998). *Environmental Soil Physics*. California (USA): Academic Press.

Nield, D. A. & A. Bejan (2013). *Convection in porous media*. Springer Science and Business Media, New York (USA).

Rohsenow, W. R. & H. Y. Choi (1961). *Heat, mass and momentum transfer*. Series in Engineering of the Physical Sciences. Prentice-Hall, Englewood Cliffs, NJ (USA).

SA (2003). AS1289.5.2.1.-2003. Methods of testing soils for engineering purposes. Method 5.2.1: Soil compaction and density testsDetermination of the dry density/moisture content relation of a soil using modified compactive effort.

Smith, J. C. & C. E. Augarde (2013). Optimum water content tests for earthen construction materials. *Construction Materials ahead of print*.